Available online at www.sciencedirect.com
SCIENCE DIRECT®
Journal of Catalysis 220 (2003) 161–171
JOURNAL OF CATALYSIS
www.elsevier.com/locate/jcat

Synergistic effect in the hydroxylation of phenol over CoNiAl ternary hydrotalcites

Vicente Rives,[a] Olga Prieto,[a] Amit Dubey,[b] and Srinivasan Kannan [b,*]

[a] *Departamento de Química Inorgánica, Universidad de Salamanca, 37008 Salamanca, Spain*
[b] *Silicates and Catalysis Discipline, Central Salt and Marine Chemicals Research Institute, Bhavnagar 364 002, India*

Received 24 February 2003; revised 9 May 2003; accepted 27 May 2003

Abstract

Hydroxylation of phenol was carried out over a series of CoNiAl ternary hydrotalcites (HTs) having a (Co + Ni)/Al atomic ratio close to 2.6 and a Co:Ni atomic ratios ranging from 1:0 to 0:1 using H_2O_2 as oxidant and water as solvent. Both end members of this series, namely CoAl-HT and NiAl-HT, showed negligible conversion of phenol, while cooperative catalytic behavior was noted when both elements were present together. However, activity of the catalysts varied with Co/Ni atomic composition, wherein the activity decreased with a decrease in the concentration of cobalt. A variation in the activity with the crystallinity of the materials was noted wherein a highly ordered material showed maximum activity and dropped with a decrease in the orderliness of the layered structure. Temperature-programmed reduction (TPR) of the fresh samples substantiated the activity trend by exhibiting a decrease in the reduction maximum with a decrease in the concentration of cobalt. Probably an optimal configuration of sites involving cobalt, nickel, and Brønsted basic hydroxyl groups is necessary for promoting the reaction. Among the catalysts studied, catalyst with a Co/Ni atomic ratio of 1:5 showed maximum conversion of phenol (14.2%, substrate:oxidant = 2:1, 65 °C) with a catechol/hydroquinone ratio of 3.8. Heating of these samples even at slightly elevated temperatures (>120 °C in air for 5 h) led to complete loss in the activity necessitating the requirement of a well-ordered network. Prior to catalytic studies, the samples were characterized by various physicochemical techniques for structure–activity relationships.

Keywords: Hydroxylation of phenol; CoNiAl hydrotalcite; Synergism; Temperature-programmed reduction; Ordered network; Powder X-ray diffraction

1. Introduction

Hydroxylation of phenol is an industrially important reaction as the products, namely catechol and hydroquinone, are widely used as photography chemicals, antioxidants, polymerization inhibitors, and flavoring agents and in medicine [1]. Heterogeneous hydroxylation of phenol using H_2O_2 as oxidant over titanium silicalite by Enichem has opened vistas for environmentally benign approaches for selective oxidation/hydroxylation reactions [2]. In continuation, efforts were made to use various microporous materials, especially those containing transition metal ions for hydroxylation of phenol. Although stronger efforts were focused on titanium [3], copper [4–6], and iron-containing catalysts [7,8] for this reaction, little importance was given to nickel [9] and cobalt-containing systems [10]. Dai et al. [10] studied substitution of transition metal ions for aluminum and/or phosphorus in the $AlPO_4$-11 framework and tested for phenol hydroxylation. Among the metal ions studied, iron showed the maximum activity, followed by cobalt and manganese. CoAPO-11 showed 23% conversion with a nearly catechol to hydroquinione ratio of 1:1 using a 1:0.9 substrate:oxidant mole ratio at 80 °C. Among various CoAPOs studied with varying pore sizes, CoAPO-11 showed the maximum conversion despite its smaller pore size, suggesting that the active sites are on the external surface of the catalyst. Very recently, Maurya et al. [11] showed that, among several metal (Cr, Fe, Ni, Zn, and Bi) salpn complexes (*N*, *N*-bis(salicylidene)propane-1,3-diamine; (H_2Salpn)) encapsulated in zeolite, Ni(salpn)-Y showed the lowest performance for oxidation of phenol. Hydrotalcite-like compounds are a class of two-dimensional materials receiving increasing attention in recent years for selective oxidation reactions [12–14]. Structurally, isomorphous substitution of M^{3+} in a brucite-like lattice $M^{2+}(OH)_2$ occurs and the excess positive charge in the

* Corresponding author.
E-mail address: kanhemad1@sancharnet.in (S. Kannan).

0021-9517/$ – see front matter
doi:10.1016/S0021-9517(03)00245-8

sheets is balanced by anions occupying the interlayers along with water molecules [15]. Zhu et al. [16] carried out hydroxylation of phenol over binary hydrotalcites of the general formula M(II)Al-HT, where M(II) = Mg, Zn, Ni, and Co, using H_2O_2 as oxidant, and concluded none of them showed measurable conversion. We have disclosed in our earlier work various copper-containing hydrotalcites as potential candidates for phenol hydroxylation reactions [17–19]. In an endeavor to find new catalysts, we have attempted a noncopper-containing mixed ternary hydrotalcite where we have introduced cobalt and nickel as bivalent metal ions. The choice of the metal ions is based on their well-known redox characteristics, which may vary when they are present together and in turn can result in altered behavior. Despite the fact observed from our preliminary studies, wherein both pure cobalt and nickel-containing hydrotalcites did not show catalytic activity for phenol hydroxylation, some of the earlier reports noted below prompted us to introduce these two metal ions in HT-like lattice together to perceive any positive phenomenon occurring. It is known that matrix, concentration, and the presence of cocations associated with the system can significantly modify redox properties of the metal ions. In a report by Halawy et al. [20], dehydrogenation of isopropyl alcohol was influenced by the addition of nickel on cobalt supported on MgO. They concluded that the inclusion of nickel influenced metal–oxygen bond strength of catalyst components as well as surface basicity and in turn on the activity of the catalyst. Kaneda and co-workers [13] studied the oxidation of alcohols and aromatic compounds over RuCoAl ternary hydrotalcite using molecular oxygen as oxidant. The high activity of this catalyst was attributed to synergism derived from the interaction of cobalt and ruthenium cations in the catalyst. Among the various metal ions screened in $RuMAlCO_3$-HT (M = Co, Mn, Fe, Zn, and Mg) catalysts, cobalt resulted in a maximum yield of oxidized products. Yumin et al. [14] carried out liquid-phase oxidation of *p*-cresol to *p*-hydroxybenzaldehyde over cobalt-containing ternary hydrotalcites with the general formula $CoMAlCO_3$-HT ($M = Cu^{2+}$, Ni^{2+}, Mn^{2+}, Cr^{3+}, and Fe^{3+}) and found a maximum activity for the copper-promoted catalyst, despite the wide distribution of specific surface areas of these catalysts. Trifirò and co-workers [21] studied the influence of cobalt in a CuZnCr-ternary oxide system, wherein they observed a dramatic deactivation with a cobalt content up to 2%, but increased with a further increase in cobalt content, respectively, attributed to poisoning of the oxidizing ability of the catalyst surface and to a synergic effect. In this report, our goal was to find whether the redox behavior of the catalyst is varied when both nickel and cobalt were present together in CoNiAl ternary hydrotalcites, and to visualize whether such a phenomenon resulted in synergism, in particular for hydroxylation of phenol.

2. Experimental

2.1. Sample preparation

The samples were prepared by coprecipitation under low supersaturation. Two solutions, namely solution (A) containing the desired amount of metal (Co, Ni, Al) nitrates and solution (B) having precipitating agents (i.e., NaOH and Na_2CO_3), were added slowly (1 ml/min) and simultaneously in a four-necked round-bottomed flask fitted with a pH electrode for maintaining the pH around 9–10 during addition under vigorous stirring at room temperature. The addition took ca. 90 min and the final pH was adjusted to 10 by adding few drops of precipitant solution. The samples were aged in the mother liquor at 65 °C for 24 h, filtered off, washed (until total absence of nitrates and sodium in the washing liquids), and dried in an air oven at 80 °C for 12 h. The solids were hand-ground and exhibited a cream to green color with increasing nickel content. In all cases, the atomic ratio between the divalent and the trivalent cations was maintained around 3.0, while the Co:Ni atomic ratio was changed between 1:0 and 0:1; i.e., including end members containing only Co–Al or Ni–Al in the layers. Consequently, the samples having both nickel and cobalt are named as CoNiAlXY-HT, where XY stands for the nominal Co:Ni atomic ratios. For the sake of brevity, most of the results here reported correspond to six selected samples of this set, although complete information of all nine samples can be accessed as an electronic supplementary information data.

2.2. Techniques

Elemental chemical analysis for Co, Ni, and Al was carried out by atomic absorption in a Mark 2 ELL-240 apparatus, in Servicio General de Analisis Quimico Aplicado (University of Salamanca, Spain).

Powder X-ray diffraction (PXRD) patterns were recorded in a Siemens D-500 instrument, using Cu-K_α radiation (λ = 1.54050 Å) and equipped with AT Diffract software. Identification of the crystalline phases was made by comparison with the JCPDS files [22].

FT-IR spectra were recorded in a Perkin-Elmer FT1730 instrument, using KBr pellets; 100 spectra (recorded with a nominal resolution of 4 cm^{-1}) were averaged to improve the signal-to-noise ratio.

Temperature-programmed reduction (TPR) analysis was carried out in a Micromeritics 2900 TPD/TPR instrument. The reducing agent was H_2–Ar (5% vol) from L'Air Liquide (Spain) and the gas flow (50 ml min^{-1}), sample weight (15–20 mg), and heating schedule (10 °C min^{-1}) were chosen according to the literature [23] to optimize resolution of the curves. Calibration of the instrument was carried out with CuO (from Merck).

Thermogravimetric (TG) and differential thermal analyses (DTA) were carried out in TG-7 and DTA-7 instruments from Perkin Elmer, in flowing oxygen or nitrogen

(from L'Air Liquide, flow 50 ml min^{-1}), at a heating rate of 10 °C min^{-1}, and using alumina (from Merck) calcined at 1200 °C as a reference for the DTA studies.

Specific surface area assessment and pore-size analysis were carried out in a Gemini instrument from Micromeritics. The sample (ca. 80–100 mg) was previously degassed in flowing nitrogen at 150 °C for 2 h in order to remove physisorbed water in a FlowPrep060 apparatus, also from Micromeritics, and the data were analyzed using published software [24].

Particle-size measurements were carried out by wet dispersion technique using water as dispersant in a Malvern Mastersizer-2000 (Model-Hydro2000S) employing laser light scattering. The samples were spun at 2500 rpm for homogenization and 2000 scans were taken for averaging the measurements.

2.3. Hydroxylation of phenol

Hydroxylation of phenol was carried out in a two-neck glass reactor (50 ml) fitted with a condenser and a septum [18]. Hydrogen peroxide (30% w/v) was added through septum at once to the magnetically stirred solution of phenol containing catalyst and solvent kept at the desired reaction temperature. The course of the reaction was monitored by withdrawing periodically small samples (0.05 cm^3) and analyzed by gas chromatography (GC; Shimadzu-14B, Japan) fitted with OV-17 packed column (2 m × 4 mm i.d.) using a flame ionization detector. Quantification was done after considering response factors of both reactants and products derived using standard mixtures.

3. Results and discussion

3.1. Elemental chemical analysis

The results obtained are summarized in Table 1, together with the formulae calculated for the samples. The carbonate content was calculated from M^{II}/Al atomic ratios, assuming carbonate is the only charge-compensating interlayer anion balancing the positive charge in the layers (because of the presence of aluminum) and the oxidation state of Co^{2+} is unaffected during the synthesis procedure, in agreement with other experimental results (see below); the interlayer water content was calculated from the TG curves. The M^{II}/Al and Co/Ni ratios in the solids were reasonably coincident with the ratios in the starting solutions; the small deviation observed is rather common and has been usually ascribed to a preferential precipitation of one or another cation as hydroxide [25]. Nevertheless, it should be noted that the M(II)/Al ratio in the solids were always close to 2.6–2.7, despite that the value in the starting solution was 3.0 in all cases. Deviations between the Co/Ni ratios in the solutions and in the solids are insignificant in most of the cases. The particle sizes of the samples synthesized were around 15–20 μm, except for CoNiAl91-HT, which showed around 34 μm.

3.2. Powder X-ray diffraction

The powder X-ray diffraction patterns of representative original samples are shown in Fig. 1. They show the presence of a pure hydrotalcite-like phase, without cocrystallization of any detectable impurity. Assuming a 3R packing of the layers [26–28], the harmonics close to 2θ (Cu-K_α) = 11, 24, and 35° (spacings close to 7.6, 3.76, and 2.53 Å, respectively) are ascribed to diffraction by basal planes (003), (006), and (009). The basal peaks (as well the peaks in the 2θ region 60–65°) become sharper and stronger as the nickel content is increased and this effect is also observed in the PXRD diagrams of other samples included in the present study, suggesting an increase in the crystallinity of the solids; in fact, this effect can also be observed by comparing the raw intensity of the main diffraction maximum (Fig. 1, inset), as the diagrams were recorded during the same session and under identical experimental conditions. In fact, a closer look at the figure indicates, among the samples studied, that the maximum crystallinity is possessed by CoNiAl15-HT.

Lattice parameter c was calculated from the position of the first basal peak as $c = 3d_{(003)}$, and the calculated values are included in Table 1. This parameter is generally related to the coulumbic forces between the layers and the interlayer anion; as the M^{II}/Al^{III} ratio in all these six samples is the same, no variation in the c parameter is expected; actually, the mean value recorded is 22.99 Å and the maximum deviation from this value is only 0.41 Å. The first peak of the doublet close to 2θ (Cu-K_α) = 60° is due to diffraction by planes (110), and its spacing corresponds to half of the lattice parameter a, which coincides with the closest M–M distance

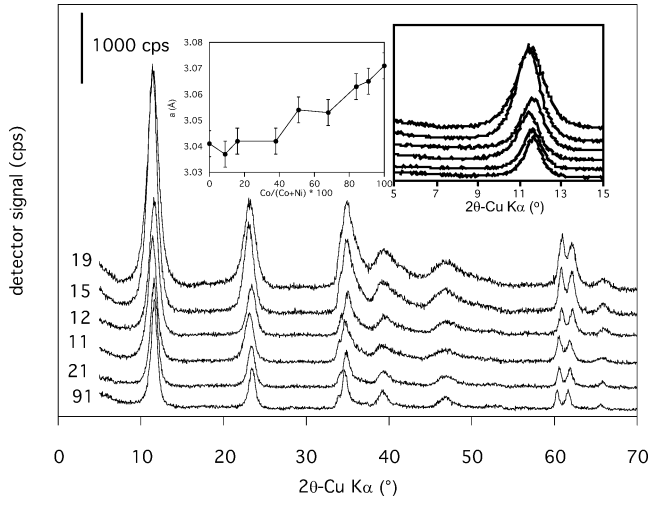

Fig. 1. Powder X-ray diffraction patterns of CoNiAl ternary hydrotalcites; inset, (right) d_{003} intensity, order of samples as in the main figure; (left) Vegard's law; 19 represents CoNiAl19-HT (figures were vertically displaced for clarity; top to bottom with increasing cobalt concentration).

Table 1
Elemental chemical analysis results, chemical formulae and lattice parameters of the samples

Sample	Co[a]	Ni[a]	Al[a]	M^{II}/Al[b]		Co/Ni[b]		Formula[c]	c/Å	a/Å
				Solution	Solid	Solution	Solid			
CoAl-HT	35.9	0	6.1	3.0	2.7	1:0	1:0	$[Co_{0.73}Al_{0.27}(OH)_2](CO_3)_{0.14} \cdot 0.40\ H_2O$	22.92	3.071
CoNiAl91-HT	32.4	3.1	6.1	3.0	2.7	9:1	10.4:1	$[Co_{0.66}Ni_{0.06}Al_{0.27}(OH)_2](CO_3)_{0.14} \cdot 0.68\ H_2O$	22.82	3.065
CoNiAl51-HT	33.4	6.3	6.8	3.0	2.7	5:1	5.3:1	$[Co_{0.61}Ni_{0.12}Al_{0.27}(OH)_2](CO_3)_{0.14} \cdot 0.91\ H_2O$	22.82	3.063
CoNiAl21-HT	25.6	12.0	6.6	3.0	2.6	2:1	2.1:1	$[Co_{0.49}Ni_{0.23}Al_{0.28}(OH)_2](CO_3)_{0.14} \cdot 0.78\ H_2O$	22.83	3.053
CoNiAl11-HT	19.1	18.6	6.5	3.0	2.7	1:1	1.0:1	$[Co_{0.37}Ni_{0.36}Al_{0.27}(OH)_2](CO_3)_{0.14} \cdot 0.91\ H_2O$	23.12	3.054
CoNiAl12-HT	13.5	22.4	6.2	3.0	2.7	1:2	1:1.67	$[Co_{0.27}Ni_{0.45}Al_{0.27}(OH)_2](CO_3)_{0.14} \cdot 0.89\ H_2O$	22.78	3.042
CoNiAl15-HT	5.9	29.9	6.2	3.0	2.7	1:5	1:5.10	$[Co_{0.12}Ni_{0.61}Al_{0.27}(OH)_2](CO_3)_{0.14} \cdot 1.03\ H_2O$	23.18	3.042
CoNiAl19-HT	3.1	31.3	6.1	3.0	2.6	1:9	1:10.2	$[Co_{0.06}Ni_{0.66}Al_{0.28}(OH)_2](CO_3)_{0.14} \cdot 0.73\ H_2O$	23.05	3.037
NiAl-HT	0	33.5	5.8	3.0	2.6	0:1	0:1	$[Ni_{0.73}Al_{0.27}(OH)_2](CO_3)_{0.14} \cdot 0.77\ H_2O$	23.40	3.041

[a] Weight percentage. [b] Atomic ratio. [c] Values rounded to two significant figures.

in the brucite-like layers, whose values are also included in Table 1. With only minor deviations, *a* parameter increased with an increase in the cobalt content in the sample, in agreement with the larger ionic radius of Co^{2+} (0.74 Å) with respect to Ni^{2+} (0.72 Å) in an octahedral, high spin, environment [29]. A rather linear increase in *a* is observed as the molar Co/(Co + Ni) ratio is increased (Al^{3+} has been ignored, as its molar fraction is almost constant in all nine samples studied), indicating the compliance of Vegard's rule (Fig. 1, inset).

3.3. FT-IR spectroscopy

Although all samples show rather similar spectra (Fig. 1, electronic supplementary, material, text), subtle differences can be noted. A broad intense band is recorded around 3450 cm^{-1} and is due to ν_{OH}-stretching mode of hydroxyl groups from the layers and the interlayer water molecules; broadening arises from extended hydrogen bonding. A closer look at this vibration mode indicates a shift in the ν_{OH} band position to larger wave numbers with an increase in cobalt content, possibly with lesser broadening. An analogous trend was noted for a rather weak band at 1632–1640 cm^{-1} due to the bending mode of interlayer water molecules, although the position of the band could not be further marked because of its presence as a shoulder to the stronger, rather sharp band at 1363 cm^{-1}, due to the antisymmetric ν_3 mode of interlayer carbonate anions. This band does not, however, shift irrespective of the composition of the brucite-like layers. This fact, together with the absence of any band close to 1080 cm^{-1} (position expected for the IR forbidden ν_1 mode of carbonate) suggests retention of D_{3h} symmetry of the carbonate anion in the interlayer region of the solids [30].

The main differences in the spectra are observed in the region below 1000 cm^{-1}, where the bands due to the M–OH stretching and M–OH–M′ bending modes are recorded, together with other modes of the carbonate anion. A broad band at 763 cm^{-1} with a weak shoulder centered around 861 cm^{-1}, whose intensity decreases with Co content is recorded. Kloprogge and Frost [31] have ascribed this band to translation modes of hydroxyl groups mainly influenced by trivalent aluminum [32]. The later weak shoulder is usually attributed to the ν_2 mode of the interlayer carbonate group [33]. Another absorption around 600 cm^{-1} splits into two bands around 603 and 563 cm^{-1}; the intensity of the former band also slightly decreases with a decrease in the Co content. Although it is not possible to pinpoint the band and its possible assignment as there are three elements in the hydrotalcite network, considering the variation, the high wave number band may be attributed to Co–O translation mode, while the other band may involve contributions from both Ni–OH and Al–OH translation modes [34]. Finally, a single band at 407 cm^{-1} for the Co-free sample splits into two absorptions at 421 and 390 cm^{-1}, clearly detected for the Co-rich sample [35]. Considering the above observations (shift in the ν_{OH} band position and M–OH translation mode to higher frequencies with increasing concentration/addition of cobalt), we can conclude a weaker M–OH strength in the brucite lattice with a lesser extent of hydrogen bonding for cobalt-containing samples.

3.4. Thermal analyses (TG and DTA)

These studies were carried out both in nitrogen and in oxygen, in order to detect any oxidation process ($Co^{2+} \rightarrow Co^{3+}$ oxidation is expected under oxidant conditions) occurring during calcination. The DTA curves for two representative samples, one rich in Co and another rich in Ni, are given in Fig. 2, both recorded in dynamic nitrogen and oxygen atmospheres.

The DTA curves for sample CoNiAl19-HT are almost coincident when recorded in oxygen or in nitrogen. The first endothermic effect is generally ascribed [36] to removal of interlayer water, while the second effect, which usually consists of two overlapped endothermic effects, is due to dehydroxylation of the brucite-like layers and evolution of gaseous CO_2 from interlayer carbonate anions, as confirmed in some cases by mass spectrometric analysis of the gases evolved [37]. In addition, a rather broad, extremely weak effect around 100 °C is ascribed to removal of water molecules physisorbed on the external surface of the crystallites. The

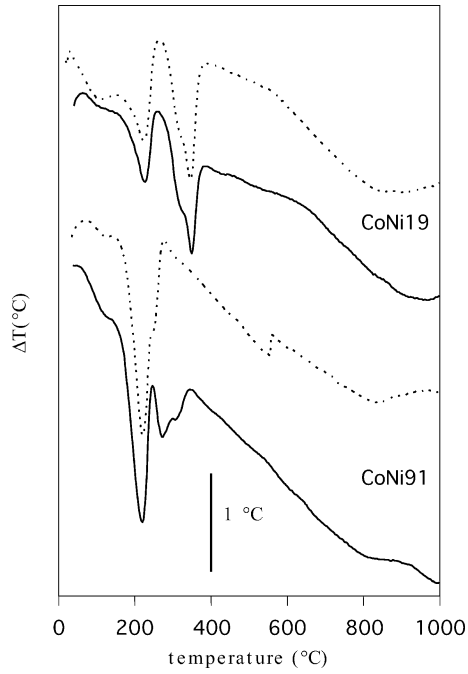

Fig. 2. Differential thermal analysis curves of CoNiAl19-HT and CoNiAl-91-HT; solid lines, nitrogen; dotted lines, oxygen (for sake of brevity samples were denoted as CoNi19 and CoNi91; 10 °C min^{-1}; alumina as reference; 50 ml min^{-1}).

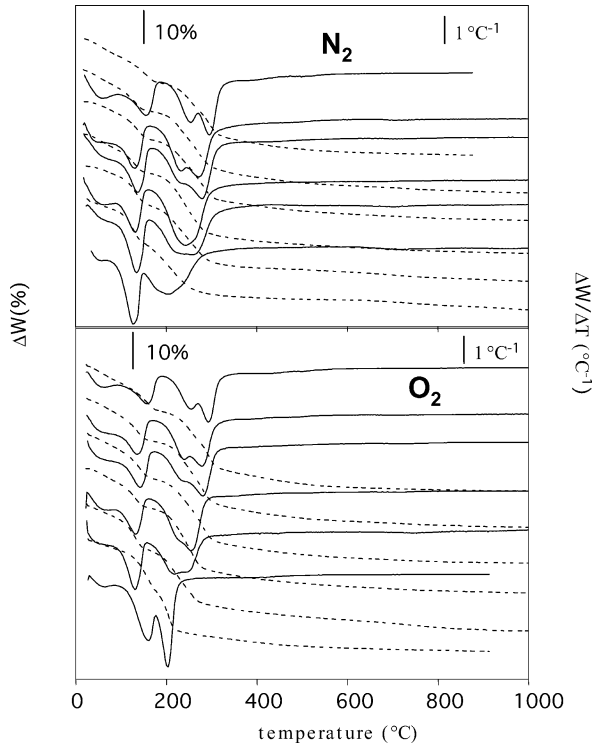

Fig. 3. Thermogravimetric (solid lines) and differential thermogravimetric (dotted lines) curves for CoNiAl-HTs recorded in (top) nitrogen and (bottom) oxygen; within each figure, bottom plots are for the sample CoNiAl91-HT and the top plots for sample CoNiAl19-HT (top to bottom with increasing cobalt concentration).

fact that both curves are coincident for this sample (they are also coincident for sample NiAl-HT) indicates that no oxidation takes place in these two samples or that it is extremely weak to be recorded by this technique.

However, important differences are observed for sample CoNiAl91-HT. In this Co-rich sample (the same differences are observed for sample CoAl-HT), although the first two endothermic effects (the broad and weak one due to removal of physisorbed water, and a sharp and intense one due to removal of interlayer water, respectively) are almost coincident, the second thermal effect, which consists of, at least, two overlapped effects in nitrogen, is absolutely absent when the analysis is performed in oxygen. This behavior has been previously reported by some of us [38] for CoAl LDHs, and has been ascribed to oxidation of Co^{2+} species to Co^{3+} in an oxidant atmosphere during heating: heat released during this oxidation cancels heat absorption required to produce water and carbon dioxide from layer hydroxyl groups and interlayer carbonate anions, respectively. The sharp "step" around 500 °C in the curve of this sample recorded in oxygen is an instrumental artifact.

From these results for these two samples with "extreme" chemical compositions, it is clear that the use of one or another reaction atmosphere affects the chemical processes occurring during heating, and when analyzing the results for the other seven samples studied, it is found that the behavior changes smoothly as the Co/Ni molar ratio is changed.

The TG curves recorded both in nitrogen and in oxygen are included in Fig. 3. Although the integral (TG) curves show some changes in their slope, it is easier to analyze these results from the DTG curves, also included in Fig. 3. In all cases, a first weak weight loss around 100 °C, which has been previously ascribed [37] to removal of water physisorbed on the external surface of the crystallites, is recorded, in agreement with the DTA results discussed above. Then, an important weight loss, typically ca. 13% of the initial sample weight, is recorded, and it has been ascribed to removal of interlayer water molecules. A small *plateau* is recorded around 200 °C in all cases, but followed immediately by a new weight loss, which is even split into two consecutive steps, more clearly when the Ni content is increased (compare the DTG curves for samples CoNi19 and CoNi91). The average temperature of this second step shifts toward higher values as the Ni content is increased, indicating that the presence of cobalt introduces some sort of instability to these solids (cf. FT-IR results). The weight loss in this second step is ca. 20% of the initial sample weight.

The curves recorded when the analysis are carried out in oxygen (also given in Fig. 3) are different from those recorded in nitrogen, especially as the cobalt content is increased; actually, the TG and DTG curves for sample CoNi19 in nitrogen and in oxygen can be superposed (top curves of both panels in Fig. 3). However, the curve for sample CoNi91 in oxygen is absolutely different from that recorded in nitrogen, wherein a sharp, well-defined DTG minimum is recorded, instead of a broad, ill-defined effect in nitrogen. In agreement with the DTA results, these differ-

ences again confirm that Ni-rich samples lead to a similar behavior both in nitrogen and in oxygen, while Co-rich samples display different behavior, probably because of the oxidation processes noted above being evident in these cases. Total weight loss was around 38–40% in all the samples. The water content in the samples, given in Table 1, was calculated from the weight loss of the samples recorded in nitrogen, where results indicated that the oxidation states of the metal cations are preserved.

3.5. Temperature-programmed reduction

Although Al^{3+} is not reduced under the experimental conditions used in our TPR runs, both Co and Ni cations are reduced to the metallic state; we have previously demonstrated reduction of Co^{n+} to Co^0 and of Ni^{2+} to Ni^0 in LDHs [37,39]. The curves recorded are included in Fig. 4. In all cases, a first weak reduction maximum is recorded around 300 °C, but its intensity has no relationship to the chemical composition of the samples (Ni or Co content), and its origin remains obscure. Above this peak, a single, despite composed, broad reduction peak is recorded. It should be stressed that analysis of TPR curves is difficult because the sample is being decomposed while the cations are being reduced. For sample CoNiAl91-HT the maximum is recorded around 600 °C, but with an important shoulder around 450 °C. On the contrary, the absolute maximum shifted to ca. 480 °C with an increasing nickel content; however, the tail of the curve indicates the presence of a shoulder at higher temperature. From the molar concentrations of Co and Ni present in our samples, we can tentatively conclude (as no analysis of the oxidation state of the cations could be carried out along the reduction process) that Co^{2+} is reduced at higher temperature than Ni^{2+}. In other words, the reducibility of the materials increases with an increase in nickel content.

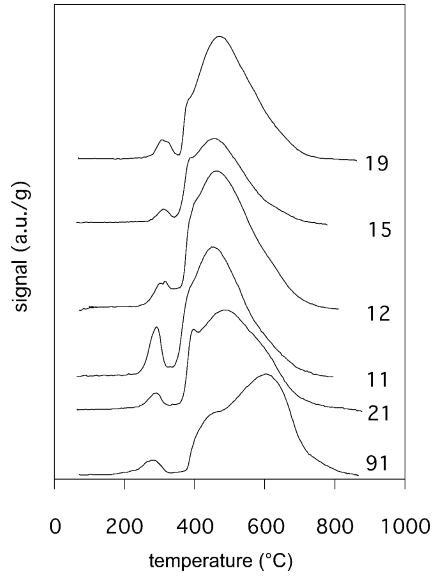

Fig. 4. Temperature-programmed reduction of CoNiAl ternary hydrotalcites; 19 represents CoNiAl19-HT.

The area under the curve is directly related to H_2 consumption during reduction, and thus, knowing the amount of reducible cations (Co^{2+} and Ni^{2+} in our case, from elemental chemical analysis) and the amount of hydrogen consumed, the original oxidation state of the cation can be determined, according to the process:

$$MO_x\ (s) + xH_2\ (g) \rightarrow M\ (s) + xH_2O\ (g).$$

In our case the calculation is slightly more difficult, as there are two reducible species (cobalt and nickel). However, taking into account the synthesis procedure followed and the experimental results reported here, the oxidation state of both cations should be +2 in all samples. As noted above, and as it can be seen in Fig. 4, both reduction processes take place in a similar temperature range and hence deconvolution of the curves is extremely difficult; consequently, determination of individual H_2 consumptions for reduction of nickel and cobalt is complex. Furthermore, reduction of a single metal cation does not necessarily takes place in a single step, and so the two overlapping peaks recorded could correspond to separate reduction of both cations (Co^{2+} and Ni^{2+}) or to overlapped reduction in more than a single step. The experimentally determined hydrogen consumption and M/H_2 ratios for all nine samples are summarized in Table 2. The values are close to 1.00, deviations being within experimental error generally accepted for this technique. In other words, each hydrogen molecule consumed corresponds to a decrease in two units in the oxidation state of the metal cations. These results confirm that the original oxidation state of the cations was +2 in all the samples prepared, confirming the lack of oxidation of Co^{2+} species during synthesis.

3.6. Surface texture

All nine samples displayed type II nitrogen adsorption isotherms at −196 °C, according to the IUPAC classification (Fig. 2, electronic supplementary, material, text) [40].

Table 2
Quantitative results from TPR experiments and summary of texture results

Original LDHs	H_2 consumption[a]	$H_2/(Co+Ni)$[b]	S_{BET}[c]	V_p[d]
CoAl-HT	6565	0.99	76	306
CoNiAl91-HT	6274	1.04	84	344
CoNiAl51-HT	6821	1.01	60	174
CoNiAl21-HT	5903	0.92	71	223
CoNiAl11-HT	6986	1.09	82	248
CoNiAl12-HT	6241	1.02	82	286
CoNiAl15-HT	6014	0.99	119	417
CoNiAl19-HT	6042	1.03	148	435
NiAl-HT	6067	1.06	99	353

[a] µmol/g. [b] Rounded values. [c] m^2/g rounded values. [d] µl liquid N_2/g.

The curves show a rather small hysteresis loop closing at P/P_0 around 0.4–0.5 (depending on the relative Co/Ni molar ratio). These curves indicate that all samples are either mesoporous or nonporous, without micropores, i.e., nitrogen molecules are unable to penetrate in the interlayer space of these hydrotalcites with rather small interlayer anions [41]. The absence of micropores is further confirmed from V–t plots [42], which showed in all cases straight lines passing through the origin upon extrapolation. The S_{BET} values, together with the total pore volumes, are summarized in Table 2. Total pore volume and specific surface area roughly decrease as the Co content is increased; probably these changes originate from a change in the morphologies of the crystallites with increasing cobalt concentration. The pore-size distribution curves show a main contribution of pores with a diameter close to ca. 35 Å, in addition to a broad and varied contribution (depending on the samples) by pores with diameters ranging from 25 to 100 Å.

3.7. Hydroxylation of phenol

Table 3 summarizes the activity of various samples studied. On all catalysts, catechol (CAT) and hydroquinone (HQ) were formed as major products. Among the catalysts studied, CoNiAl15-HT showed maximum conversion of phenol (14.2%) with a CAT/HQ ratio of around 3.8. A closer look at the data indicates an increase in the conversion of phenol (with a preference of catechol formation) with an increase in concentration of nickel, up to a level and decreased with a further increase in the concentration. It should be noted here that both end members, namely CoAl-HT and NiAl-HT (Co/Al atomic ratio of 3.0 and Ni/Al atomic ratio of 3.0, respectively), were inactive for hydroxylation of phenol. The most active catalyst (CoNiAl15-HT) was taken for further study.

Influence of substrate:catalyst ratio indicated an interesting observation wherein no conversion was noted at higher catalyst concentrations (substrate:catalyst ratio (w/w), 10:1, 20:1, and 40:1). A sharp increase in the conversion (14.2%) was noted when a much higher substrate:catalyst ratio of 100:1 was employed. However, conversion decreased with a further increase in this ratio (6% for 200:1 ratio). A substrate:catalyst ratio of 100:1 was then selected for further studies. In order to identify the influence of the reaction medium on phenol hydroxylation, reaction was performed in various solvents (apart from water), namely, acetone, acetonitrile, t-butanol, tetrahydrofuran (THF), and dimethylformamide (DMF). None of the solvents other than water showed measurable conversion. Furthermore, when the reaction was carried out using different oxidants other than H_2O_2, namely, oxygen, air, and t-butylhydroperoxide, none of these oxidants was able to hydroxylate phenol to a significant extent under similar reaction conditions. Variation in the reaction temperature (30 to 90 °C) for the reaction showed that the conversion increased with the temperature up to 65 °C, while a further increase in the temperature decreased the conversion of phenol. This could probably be due to competitive thermal decomposition of H_2O_2 at higher temperatures. However, at all temperatures catechol is preferred, more so if the conversion of phenol is lower. Fig. 5 shows the effect of reaction time on the conversion of phenol over CoNiAl15-HT. It is clear that no conversion was observed up to 4 h (at 65 °C), but conversion increased with an increase in time up to 24 h. No significant variation in the conversion (and CAT/HQ ratio) was noted even when the reaction was allowed up to 120 h. Variation of substrate:oxidant ratio indicated that the conversion increased with a decrease in the ratio, the values are summarized in Table 4. Furthermore, an increase in conversion is nearly proportional to an increase in H_2O_2 concentration, maintaining a similar selectivity for dihydroxybenzenes.

In order to perceive the effect of calcination temperature on hydroxylation of phenol, CoNiAl15-HT was calcined at different temperatures (150, 400, 600, and 800 °C) for 6 h in air. No activity was observed for the calcined catalysts at all temperatures. Further, in a closer study, the sample was calcined at 100–180 °C for 6 h in air and studied for phenol hydroxylation. The sample calcined at 100 °C showed around 13.2% conversion (similar to the fresh sample) with a CAT/HQ ratio of around 4.0, while all other catalysts calcined above 100 °C showed no conversion of phenol.

Table 3
Phenol hydroxylation activity of CoNiAl ternary hydrotalcites[a]

Catalyst	Conversion	Product distribution (%)		
	(%)	CAT	HQ	CAT/HQ
CoAl-HT	0	0	0	–
CoNiAl91-HT	5.0	100	0	∞
CoNiAl21-HT	7.6	100	0	∞
CoNiAl11-HT	8.6	100	0	∞
CoNiAl12-HT	8.9	100	0	∞
CoNiAl15-HT	14.2	79	21	3.8
CoNiAl19-HT	4.0	100	0	∞
NiAl-HT	0	0	0	–

[a] Phenol, 1.0 g; phenol/H_2O_2 (mol), 2.0; catalyst, 10 mg; solvent, water (10 ml); temperature, 65 °C; time, 24 h; pH 5. CAT, catechol; HQ, hydroquinone.

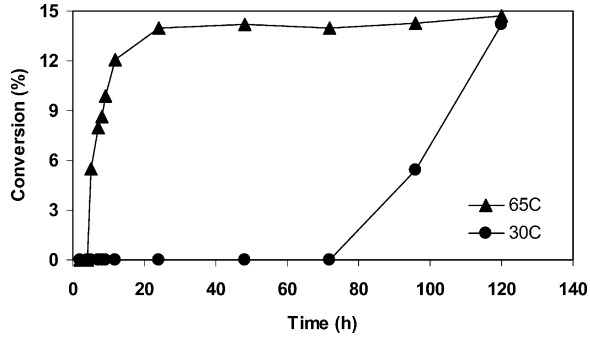

Fig. 5. Effect of reaction time on phenol conversion over CoNiAl15-HT (conditions as given in Table 3).

Table 4
Effect of the substrate:oxidant mole ratio on phenol hydroxylation activity over CoNiAl15-HT (conditions as in Table 3)

Sub:Oxi	Conversion	Product distribution (%)		
	(%)	CAT	HQ	CAT/HQ
3:1	7.5	100	0	∞
2:1	14.2	79	21	3.8
1:1	32.5	78	22	3.5
1:2	49.2	77	23	3.4

3.8. Structure–activity–property relationships

Phenol hydroxylation over CoNiAl ternary fresh hydrotalcites yielded catechol and hydroquinone with a preference to catechol. No other products were observed by GC, indicating no transitory formation of *p*-benzoquinone. This is in contrast to the results we have earlier reported for copper-containing hydrotalcites [17,18] where we observed both catechol and hydroquinone to significant levels, suggesting the nature of cations in the brucite-like sheets in influencing the course of the reaction. Although both nickel and cobalt separately in a binary hydrotalcite with aluminum as trivalent cation showed no conversion of phenol, their simultaneous presence resulted in activity, suggesting a cooperative phenomenon between cobalt and nickel in HT-like lattice in promoting the reaction. A closer look at the conversion variation indicates that with an increase in the concentration of nickel, an increase in the conversion was noted wherein maximum conversion was observed for CoNiAl15-HT (∼14%). To our knowledge, this is the best catalyst reported in the literature so far over cobalt and nickel-based catalysts for this reaction [10]. However, conversion dropped for CoNiAl19-HT. A look at the crystallinity variation indicates a similar trend wherein crystallinity increased with an increase in nickel concentration until CoNiAl15-HT and decreased with a further increase in nickel concentration. The increase in ordering upon addition of nickel in brucite-like sheets could (pure NiAl-HT is more crystalline than pure CoAl-HT; Fig. 3, electronic supplementary, material, text), probably due to the larger stabilization energy of Ni^{2+} in an octahedral geometry. In other words, the conversion has a significant dependence on the ordering of the brucite-like layers. We believe an appropriate geometry and concentration of nickel and cobalt ions in a well-ordered two-dimensional lattice could be responsible for the observed activity. However, one would also have to consider the Brønsted basic hydroxyls at the brucite sheets in influencing the reaction. This is in accordance with the results of Choudary et al. [43] who claimed activation of molecular oxygen over pure NiAl hydrotalcite for oxidation of allylic and benzylic alcohols, wherein higher specific activity was noted for NiAl2-HT (Ni/Al atomic ratio of 2.0) and attributed to its excellent layered structure. Further, if one were to look at the specific surface area of our catalysts, they increased with an increase in nickel concentration. However, specific surface area alone could not be a factor as evidenced by low conversion for CoNiAl19-HT, which showed the maximum specific surface area among the samples studied. FT-IR study substantiated the observed activity variation, as it showed higher values for both ν_{OH}-stretching and bending vibrations of water molecules for CoNiAl15-HT, suggesting weaker hydrogen-bonded interactions, in other words, better layer ordering and Brønsted basicity. TPR results (Fig. 4) also confirmed the activity variation (although may not be linear), as the reducibility of the catalysts (a measure for selective oxidation reaction) increases with an increase in the nickel concentration. In other words, a better redox couple would be available in a catalyst, which has metal ions with facile reducibility and in turn can promote oxidation reaction.

An increase in the conversion of phenol with an increase in the substrate:catalyst ratio is advantageous in view of the requirement of a lower concentration of catalyst. The drop in the conversion at higher catalyst concentrations is probably due to parallel competitive catalytic destruction of H_2O_2; i.e., H_2O_2 is catalytically destroyed and is no longer available for the "sought for" reaction to undergo (reaction mixture is colorless). In order to substantiate this, independent experiments were carried out wherein two different weights of CoNiAl15-HT (10 and 100 mg) were suspended in H_2O_2 at 65 °C in water and the H_2O_2 remaining in the system was estimated after 1 and 12 h. More than 60 and 20% of H_2O_2 remained after 1 and 12 h, respectively, for 10 mg while no H_2O_2 was noted irrespective of suspended time for 100 mg, clearly suggesting a stronger effect of decomposition of H_2O_2 at higher catalyst concentrations. However, these results are in contrast to copper-containing systems [17–19], where we observed a similar trend (activity decreases with an increase in catalyst concentration), but the drop in the conversion was due to spontaneous formation of coke (reaction mixture turns dark black) at higher catalyst concentrations, obtained through consecutive reactions of primary products, blocking the active sites, and hindering the further progress of the reaction. However, when the substrate:catalyst ratio reaches a value of 100, such a decomposition is probably optimal in forming active centers that in turn promote the reaction [17–19]. A decrease in conversion with a further decrease in this ratio could be due to a decrease in the concentration of active centers involved in the reaction. In an effort to understand this better, catalyst CoNiAl15-HT was suspended in H_2O_2 at room temperature and at 65 °C (substrate:oxidant = 1:2 mole ratio) overnight and filtrate and the residue were separated and tested for hydroxylation of phenol using a fresh portion of oxidant. No conversion was observed over the residue, while 2.6% conversion (100% selectivity to catechol) was observed for the filtrate for the catalyst suspended at room temperature and no conversion was noted for both residue and filtrate for the catalyst suspended at 65 °C, which is far less when a fresh catalyst was subjected to similar reaction conditions. This probably suggests that the initial interaction of H_2O_2 with the catalyst surface generates an active surface and/or oxygen in propagating the reaction, which may not be available

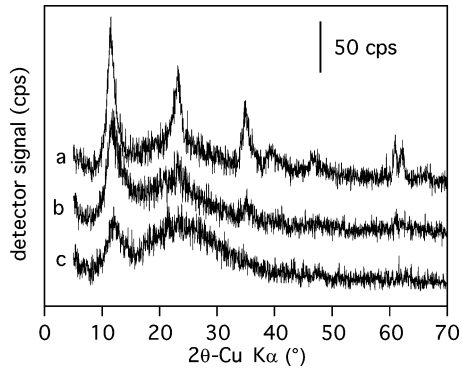

Fig. 6. Powder X-ray diffraction pattern of (a) fresh, (b) residue, and (c) used CoNiAl15-HT.

with the H_2O_2-pretreated catalyst. PXRD results, given in Fig. 6, corroborated this, as the residue showed a diffuse HT-like pattern (although the color turned to brown), but with a significant loss in the crystallinity, as evidenced from a decrease in the intensities of the basal reflections and more so with higher order *ab*-plane reflections.

An increase in conversion with an increase in H_2O_2 concentration with nearly similar selectivity for dihydroxybenzenes suggests that the added H_2O_2 is essentially used for the desired hydroxylation reaction and not for undesired consecutive reactions. Further, catechol is preferred at higher substrate:oxidant ratios, as noted for our earlier systems [17–19]. A conversion of around 50% with a CAT/HQ ratio close to 3.4 was observed for CoNiAl15-HT at a 1:2 substrate:oxidant ratio. To our knowledge, this may be the highest conversion reported so far over cobalt-based catalysts. Solvent variation studies indicated that water is the best solvent among various solvents used. We believe that the proximity of hydroxylating agent and of the substrate molecule on or near the active catalyst site is essential for driving the reaction. In water, both phenol and H_2O_2 dissolve simultaneously and can approach the active center, thereby generating the hydroxyl radicals, thought to be the active species involved in the hydroxylation reaction. Such an appropriate arrangement of molecules on the surface would be obtained if the M–OH coordination in the sheets is well ordered. Furthermore, such an electrophile is more easily produced and stabilized in water (due to hydrogen bonding) than in organic solvents. Possibly, the lack of a nonhydroxylated nature for the other organic solvents may be responsible for nonoccurrence of the reaction. The lack of reaction in the presence of other oxidants (other than H_2O_2) could possibly be due to a lack of generation of active oxidant species and the solubility problems associated with the system.

The effect of reaction time studies showed no conversion up to 4 h and then reaction occurs. Conversion increased with a further increase in reaction time up to 24 h and was unaltered until 120 h (with a similar CAT/HQ ratio), suggesting a lack of interconversion and/or consecutive reactions. The presence of induction time over these catalysts is interesting and initially catechol was formed and hydroquinone formed subsequently after 8 h. No induction period was noted for copper-containing hydrotalcites [17–19]. An experiment was carried out to ensure the presence of induction time by adding the catalyst after 4 h of reaction and monitoring the further progress of the reaction. A similar observation of induction time of around 4 h was noted. This is similar to the observation of Figueras and co-workers [44] who reported a delay in hydroxylation of phenol over silica–alumina solid acids, with catechol being the first dihydroxybenzene produced. However, they observed *p*-benzoquinone as a transitory intermediate, which we have not observed for our catalysts under our reaction conditions. An interesting observation was noted when we studied the effect of reaction time over CoNiAl15-HT at room temperature ($\sim 30\,^{\circ}C$) where conversion was not noted until 72 h, while it increased with an increase in time, and a value close to 14.0% conversion was reached after 120 h of reaction time. A further increase in time (up to 360 h) did not significantly alter the conversion of phenol. It is to be noted here that no conversion was noted at both 65 °C and at room temperature for 24 and 120 h, respectively, in the absence of catalyst. These results may indicate the kinetic dependence of induction time wherein the time is lowered with an increase in reaction temperature. Further, it has been earlier envisaged by Germain et al. [45] that addition of catechol or hydroquinone removes the induction period for faujasite FAU 2.5 ($Si/Al = 2.5$) and this was attributed to the initial oxidation of the additive in generating an autocatalytic quinonic redox couple. However, when we added catechol (20:1 mole ratio of phenol:catechol) to the initial reaction mixture (in an anticipation to see whether it has any influence on the induction time), no reduction in the induction time was noted and, in addition, conversion decreased (6.0 with 100% selective to catechol in opposition to 14.2% conversion). This confirms the nonoperation of redox mechanisms involving hydroquinone/*p*-benzoquinone. In order to unravel this phenomenon of induction time, the catalyst CoNiAl15-HT was suspended in H_2O_2 for various time intervals in H_2O at 65 °C and the residue obtained was filtered and washed and PXRD and FT-IR were done (Fig. 4 and Fig. 5, electronic supplementary, material, text). PXRD showed a progressive decrease in the crystallinity with an increase in time. In other words, long range ordering is reduced, suggesting a partial destruction of the layered structure probably through release of metal ions from the metal hydroxide sheets. We would like to ascertain here that the reaction is not occurring due to release of metal ions from lattice (homogeneous reaction), which are well known for decomposing H_2O_2 as evidenced from independent experiments noted above. In addition, FT-IR corroborated variations in both ν_{OH} stretching and additional bands around 1530 cm^{-1} after 8 h of suspended time (other samples after 1 and 4 h were similar to fresh sample), suggesting some structural variations probably through conversion of CO_3^{2-} to bicarbonates and/or hydroxy intercalation along with carbonate. Such a defective environment with altered structural characteristics (in turn with varied

acid–base properties) may provide better access for reactant and/or oxidant molecules than an ordered structure, resulting in conversion of phenol.

Our earlier results on copper-containing hydrotalcites [17–19] showed some conversion for calcined samples, however, varied with the calcination temperature, although lesser compared to fresh hydrotalcites. In the case of CoNiAl ternary hydrotalcites, no activity was observed for all catalysts calcined at different temperatures (temperatures were chosen based on the thermal properties of the materials). PXRD showed mixed metal oxide patterns where the composition of the phase is in relation to the Co/Ni atomic composition (Fig. 6, electronic supplementary, material, text). Details of the characterization of thermally calcined products will be reported elsewhere. The observed result indicates that the reaction requires a well-ordered HT-like network. Destruction of this network leads to complete loss in the activity. Surprisingly, no conversion was noted for the sample calcined at 120 °C (although sample calcined at 100 °C showed activity similar to fresh catalyst). We believe that there is a disturbance of the sheets more so near the edges, where the reactions are likely to occur, and in turn might not result in appropriate arrangement of reactants and catalyst centers. Thermal analysis of this sample showed an onset of decomposition in air at 120 °C itself and hence may lead to disorder and in turn to loss of activity. However, when the decomposition was carried out under nitrogen the temperature of the first stage of decomposition shifted to a higher temperature. To check whether this difference in thermal stability depending on the nature of the atmosphere and/or any changes in the acid–base characteristics of the catalyst is responsible for the drop in the conversion, the sample was calcined at both 120 and 140 °C under nitrogen for 2 h, and the reaction was subsequently carried out under nitrogen without exposing the calcined catalyst to atmosphere. A conversion of 2 and 0% was observed, respectively, for these samples, suggesting that even subtle disturbances in the layered network result in an altered geometric environment with a possible alteration of acid–base behavior, responsible for the drop in activity.

Considering the mechanism of hydroxylation reaction over these materials, we believe a mechanism similar to Fenton's reaction where hydroxyl radicals are likely to participate as an electrophilic agent [46]. To verify the participation of hydroxyl radicals, a study where addition of ethanol, a well-known scavenger of hydroxyl radical, was done and the conversion of phenol was monitored for CoNiAl15-HT. A decrease in the conversion was observed with increasing alcohol concentrations, with 4.5% conversion for 9:1 v/v ratio of water:ethanol while a further decrease in this ratio resulted in no conversion. Tentatively, interaction of H_2O_2 with a center composing Co–OH–Ni generates a OH radical which then reacts with phenol to produce dihydroxylated benzene.

4. Conclusions

Hydroxylation of phenol was carried out over a series of CoNiAl ternary hydrotalcites having a (Co + Ni)/Al atomic ratio close to 2.6 and Co:Ni atomic ratios ranging from 1:0 to 0:1, using H_2O_2 as oxidant and water as solvent. Although, both end members of this series, namely CoAl-HT and NiAl-HT, showed no conversion of phenol, synergistic effects operate when both metal ions are present together in the HT-like network, and among the catalysts studied, CuNiAl15-HT showed the maximum conversion of phenol (14.2%, substrate:oxidant = 2:1, 65 °C) with a catechol/hydroquinone ratio of 3.8. To our knowledge, this is the best catalyst reported in the literature so far for this reaction based on cobalt and nickel catalysts. The observed trend in the activity could be correlated to crystallinity of the materials, as the sample with the highest crystallinity (i.e., that with better ordering of the sheets) showed maximum conversion. Temperature-programmed reduction of the fresh samples substantiated the activity trend by exhibiting a decrease in the reduction maximum with a decrease in the concentration of cobalt. We believe an optimal configuration of sites involving cobalt, nickel, and Brønsted basic hydroxyl groups is necessary for promoting the reaction. In addition, carbonate present in the surface of the microcrystals may also act as a Brønsted base and may be involved in the reaction pathway. Heating of CoNiAl15-HT even at slightly elevated temperatures (above 120 °C in air) led to a complete loss in the activity because of the lack of a well-ordered network. A radical mechanism wherein participation of hydroxyl radicals as an electrophile in driving the reaction is proposed [17,18].

Acknowledgments

V.R. and O.P. thank Mr. A. Montero for his assistance in obtaining some of the experimental results, and to MCyT (Grant MAT2000-1148-C02-01) for financial support. S.K. thanks the Council of Scientific and Industrial Research, New Delhi, and Indian National Science Academy, New Delhi (BS/YSP-22), for financial assistance granted under Young Scientist Schemes. A.D. thanks the Council of Scientific and Industrial Research, New Delhi, for a Senior Research Fellowship.

References

[1] M. Howe-Grant (Ed.), Kirk-Othmer Encyclopedia of Chemical Technology, 4th ed., Wiley, 1995, p. 996.
[2] M. Taramasso, G. Perego, B. Notari, US patent 4410501, 1983.
[3] J.A. Martens, Ph. Buskens, P.A. Jacobs, Appl Catal. A 99 (1993) 71.
[4] Z. Fu, J. Chen, D. Yin, L. Zhang, Y. Zhang, Catal. Lett. 66 (2000) 105.
[5] J. Sun, X. Meng, Y. Shi, R. Wang, S. Feng, D. Jiang, R. Xu, F.-S. Xiao, J. Catal. 193 (2000) 199.
[6] F.-S. Xiao, J. Sun, X. Meng, R. Yu, H. Yuan, J. Xu, T. Song, D. Jian, R. Xu, J. Catal. 188 (2001) 273.

[7] D. Wang, Z. Liu, F. Liu, X. Ai, X. Zhang, Y. Cao, J. Yu, T. Wu, Y. Bai, T. Li, X. Tang, Appl. Catal. A 174 (1998) 25.
[8] C. Xiong, Q. Chen, W. Lu, H. Gao, W. Lu, Z. Gao, Catal. Lett. 69 (2000) 236.
[9] A. Alejandre, F. Medina, P. Salagre, A. Fabregat, J.E. Sueiras, Appl. Catal. B 18 (1998) 307.
[10] P.-S. Dai, R.H. Petty, C.W. Ingram, R. Szostak, Appl. Catal. A 143 (1996) 101.
[11] M.R. Maurya, S.J.J. Titinchi, S. Chand, I.M. Mishra, J. Mol. Catal. A 180 (2002) 201.
[12] B.F. Sels, D.E. De Vos, P.A. Jacobs, Catal. Rev.—Sci. Eng. 43 (2001) 443.
[13] T. Matsushita, K. Ebitani, K. Kaneda, J. Chem. Soc., Chem. Commun. 265 (1999).
[14] L. Yumin, L. Shetian, Z. Kaizheng, Y. Xingkai, W. Yue, Appl. Catal. A 169 (1998) 127.
[15] V. Rives (Ed.), Layered Double Hydroxides: Present and Future, Nova Science, New York, 2001.
[16] K. Zhu, C. Liu, X. Ye, Y. Wu, Appl. Catal. A 168 (1998) 365.
[17] A. Dubey, V. Rives, S. Kannan, Phys. Chem. Chem. Phys. 3 (2001) 4826.
[18] A. Dubey, V. Rives, S. Kannan, J. Mol. Catal. A 181 (2002) 151.
[19] A. Dubey, S. Velu, E. Suzuki, S. Kannan, Appl. Catal. A 238 (2003) 319.
[20] S.A. Halawy, M.A. Mohamed, S.F. Abd El-Hafez, J. Mol. Catal. 94 (1994) 191.
[21] G. Fornasari, A.D. Huysser, L. Mintchev, F. Trifirò, A. Vaccari, J. Catal. 135 (1992) 386.
[22] Joint Committee on Powder Diffraction Standards, International Centre for Diffraction Data, Pennsylvania, 1977.
[23] P. Malet, A. Caballero, J. Chem. Soc., Faraday Trans. I 84 (1988) 2369.
[24] V. Rives, Adsorpt. Sci. Technol. 8 (1991) 95.
[25] J.M. Fernández, C. Barriga, M.A. Ulibarri, F.M. Labajos, V. Rives, Chem. Mater. 9 (1997) 312.
[26] A.S. Bookin, V. Cheskashin, V.A. Drits, Clays Clay Miner. 41 (1993) 558.
[27] A.S. Bookin, V.A. Drits, Clays Clay Miner. 41 (1993) 551.
[28] V.A. Drits, A.S. Bookin, in: V. Rives (Ed.), Layered Double Hydroxides: Present and Future, Nova Science, New York, 2001, Ch. 2, p. 39.
[29] R.D. Shannon, C.T. Prewitt, Acta Crystallogr. B 25 (1969) 925.
[30] F.M. Labajos, V. Rives, M.A. Ulibarri, J. Mater. Sci. 27 (1992) 1546.
[31] J.T. Kloprogge, R.L. Frost, J. Solid State Chem. 146 (1999) 506.
[32] J. Perez-Ramirez, G. Mul, J.A. Moulijn, Vib. Spectrosc. 27 (2001) 75.
[33] J.T. Kloprogge, R.L. Frost, Appl. Catal. A 184 (1999) 61.
[34] M.J. Hernández-Moreno, M.A. Ulibarri, J.L. Rendón, C.J. Serna, Phys. Chem. Miner. 12 (1985) 34.
[35] J.T. Kloprogge, R.L. Frost, in: V. Rives (Ed.), Layered Double Hydroxides: Present and Future, Nova Science, New York, 2001, Ch. 5, p. 139.
[36] V. Rives, Inorg. Chem. 38 (1998) 406.
[37] V. Rives, in: V. Rives (Ed.), Layered Double Hydroxides: Present and Future, Nova Science, New York, 2001, Ch. 4, p. 115.
[38] M.A. Ulibarri, J.M. Fernández, F.M. Labajos, V. Rives, Chem. Mater. 3 (1991) 626.
[39] V. Rives, M.A. Ulibarri, A. Montero, Appl. Clay Sci. 10 (1995) 83.
[40] K.S.W. Sing, D.H. Everett, R.A.W. Haul, L. Moscou, R. Pierotti, J. Rouquerol, T. Sieminiewska, Pure Appl. Chem. 57 (1985) 603.
[41] V. Rives, in: V. Rives (Ed.), Layered Double Hydroxides: Present and Future, Nova Science, New York, 2001, Ch. 8, p. 229.
[42] B.C. Lippens, J.H. de Boer, J. Catal. 4 (1965) 319.
[43] B.M. Choudary, M. Lakshmi Kantam, A. Rahman, Ch.V. Reddy, K. Koteswara Rao, Angew Chem., Int. Ed. Engl. 40 (2001) 763.
[44] A. Germain, M. Allian, F. Figueras, Catal. Today 32 (1996) 145.
[45] M. Allian, A. Germain, F. Figueras, Catal. Lett. 28 (1994) 409.
[46] C. Walling, Acc. Chem. Res. 8 (1975) 125.